Experimental study of heat transfer inside a real scale innovative air solar collector

Catalin Sima[1*], **Catalin Teodosiu**[1], **Cristiana Croitoru**[1], **Florin Bode**[2]

[1] Technical University of Civil Engineering Bucharest,CAMBI Research Centre
[2] Technical University of Cluj-Napoca

*E-mail: simacatalin25@gmail.com

The study is performed on a glazed transpired solar collector, investigating the effect of different distances between the glazing and the absorber (30, 50, 70, and 100 mm) for different airflow values. The results show that the best solution among the tested configurations is with 30 mm distance between the glazing and absorber, no matter what the air flow rate is. The efficiency of the GTC in this case is 16-19% higher for air flow rates around 100 m3/h,m2 and even 30-40% higher for air flow rates around 150-200 m3/h, m2 – compared to configurations with larger distance between the glazing and absorber.

1. Introduction

One of the most used cost-effective equipment, in order to collect solar energy, is the solar air or water collector. According to Reichl et al. [1], when using a solar air collector instead of a solar water collector the overall costs are lower, the environmental impact is lower and during the cold periods there is no risk of freezing. Moreover, by using an air solar collector we can obtain outlet temperatures up to 65 °C, temperature values suitable for building applications [2]. Air solar collector can be opaque or transparent, plate or transpired, with or without integrated energy storage [3]. According to the comprehensive literature study conducted , TSC can be used for passive cooling, building heating, drying applications, fresh air preheating, greenhouses projects thus reducing operating costs, energy consumptions for heating and cooling and enhancing the indoor comfort [4-7]. There are several types of solar air collectors [8, 9] but mainly, solar air collectors could be classified as: glazed solar collectors and transpired solar collectors .

Due to architectural or thermal constraints for example, these systems have not been widely used in residential projects, while optimisation studies are still needed. Intensive parametrical research studies have been dedicated to optimisation process regarding the shape of the orifices [10, 11] or the pattern [12], while other concentrated to different configurations, introducing protective layers like glazed surfaces. TSCs depend on meteorological parameters in a high amount, especially on the wind speed [12, 13]. Glazed solar air collectors (GSC) are independent of weather conditions (wind speed, wind direction, precipitation etc.) because of the glazed cover, thus the use of glass sheets in front of the solar collector help increasing the air temperature inside the solar collector and leading to a better overall efficiency[14, 15]. Glazed solar air collectors (GSC) are recommended because of their efficiency, their higher rise in temperature and reduced operating costs.

In this article we have studied a glazed transpired solar collector (GTC) which is composed of a perforated metal sheet covered by a glass panel. Two different configurations were tested, while measuring the results for different air flow rates.

2. Air solar collector experimental set-up

The experimental set-up consists of a real scale glazed transpired solar collector (GTC) – Figure 1. As a result, this contains a glazing of 4 mm thickness that covers a classic transpired solar collector (TSC) configuration. The absorber is represented by a metal plate, perforated according to the sketch in Figure 1 (square slits of 50 x 50 mm, with uniform vertical and horizontal pitch of 50 mm). This regular array of perforations has been chosen as it has been demonstrated that the geometry and the arrangement of absorber's perforations do not play a determinant role on the GTC performance[16].

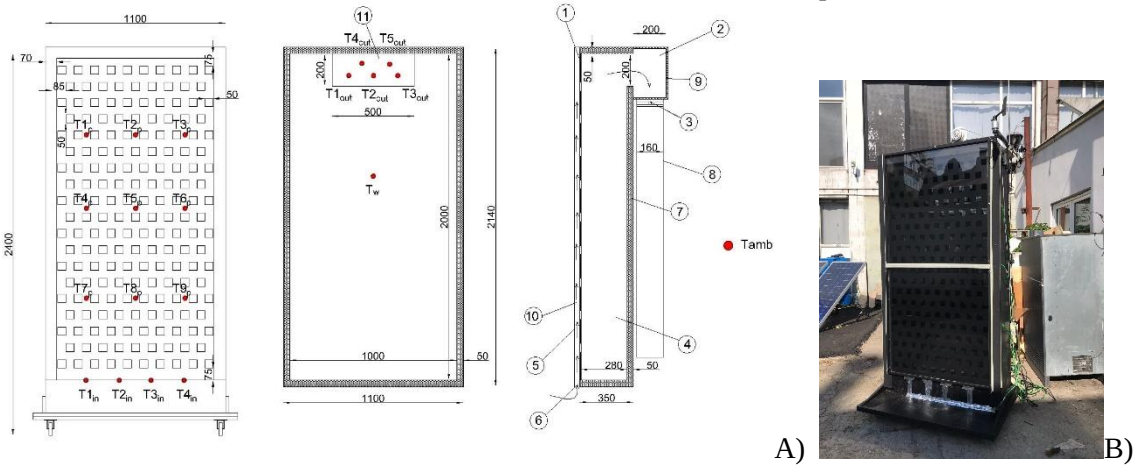

Figure 1. A) Scheme of the experimental glazed transpired solar collector 1 – transpired plate; 2 – plenum; 3 – fan; 4 – inner cavity; 5 – glazing; 6 – air inlet; 7,9 – thermal insulation; 8 – air duct; 10 – air opening between glass and absorber; 11 – air outlet. B) Experimental glazed transpired solar collector

The circulation of the air through the GTC takes place as follows: first, the air goes into the space between the glazing and the absorber at the bottom, then the air enters through the hollows of the absorber and finally arrives into the space between the absorber and the back wall of the solar collector. Lastly, the heated air is blown by a DC fan into a duct. The fan used in the experimental investigations was controlled by means of linear DC adjustable power supply (0-60 V). This allowed us to achieve different air flows (150-400 m^3/h) through the experimental GTC, this being one of the main goals of this study. On the other hand, we have also taken into consideration different distances between the glazing and the absorber (30, 50, 70, and 100 mm) in order to determine the best configuration for the GTC efficiency.

Concerning the measurements, these can be divided in two main categories: measurements for assessing the GTC performance and measurements for the outdoor air parameters.

The experimental investigation carried out in order to determine the GTC behaviour was mainly focused on the collector inlet and outlet air temperature, as well as absorber temperature distribution.

Consequently, the experimental devices used were the following: 4 thermocouples for the inlet air temperature (T1-4_{in} – Figure 1), 5 thermocouples for the outlet air temperature (T1-5_{out} – Figure 1); 9 thermocouples placed on the absorber (T1-9_p – Figure 1); 1 thermocouple placed on the back wall of the solar collector (T_w – Figure 1). In addition, the airflow through the experimental GTC was accurately measured, using an air flow meter (see Table 1). Furthermore, the measured weather parameters included solar radiation intensity, outdoor air temperature, wind velocity, and wind direction. The solar radiation was recorded using a pyranometer (type Almemo FLA 628 S), mounted on the top of the experimental set-up, while the other parameters were measured by means of a mobile weather station with digital sensor for temperature (type Almemo FHAD 46-C2), wind velocity sensor (type Almemo FVA 615 2) and wind direction sensor (type Almemo FVA 614).

The main specifications of all experimental instruments are shown in Table 1.

All the experimental data were continuously collected throughout the experimental protocol and automatically recorded at a time interval of 30 seconds, using two data loggers (type Almemo 710). We can see a representative picture of the experimental set-up, ready for the measurements, in Figure 1

Table 1. Information about the measuring devices

Device	Measured parameter	Type	Range	Accuracy
thermocouple	air / surface temperature	K (NiCr-Ni)	-10…+105ºC	±0.2ºC
air flow meter	air flow	FlowFinder mk2 system	10…550 m^3/h	3%
digital temp.sensor	ambient temperature	Almemo FHAD 46-C2	-20…+60ºC	±0.2ºC
cup anemometer	wind velocity	Almemo FVA 615 2	0.5…50 m/s	3%
wind vane	wind direction	Almemo FVA 614	0…360º	±5º
pyranometer	solar radiation intensity	Almemo FLA 628 S	0…1500 W/m^2	< 3%

3. Results

We present below the results for two arrangements of the experimental set-up, regarding the distance between the glazing and the perforated plate: 30 mm and 50 mm. Furthermore, different air flow rates through the air solar collector were taken into consideration for each of these two configurations: 75, 100, 125, 150, 175, and 200 $m^3/h,m^2$ (the total effective surface of the experimental solar collector being 2 m^2).

First, we show in Table 2 the values of average weather data throughout the tests. It should be mentioned that the experimental protocol for each test included daily measurements from 12:00 to 18:00. On the other hand, it was chosen to take into account only the data between 1:10 p.m. and 2:10 p.m. where the recordings revealed that the weather parameters (particularly the solar radiation) were most stable each day. As a result, the values in Table 2 represent the average of the measurements during this hour (1:10 p.m. to 2:10 p.m.).

Table 2. Mean weather data during the tests (1:10 p.m. to 2:10 p.m.)

30 mm glazing - perforated plate						
Parameter / Air flow rate ($m^3/h,m^2$)	79	101.5	125	148	177	198.5
Outdoor temperature (°C)	26.5	25.2	28.1	28.4	21.5	21.8
Solar radiation (W/m^2)	770.7	785.8	758.9	719.4	771.0	755.7
Wind speed (m/s)	0.32	0.46	0.35	0.17	0.13	0.15
50 mm glazing - perforated plate						
Parameter / Air flow rate ($m^3/h,m^2$)	77	102.5	127	151	175	
Outdoor temperature (°C)	22.6	25.1	23.7	28.4	22.8	
Solar radiation (W/m^2)	681.9	659.7	685.6	684.5	617.8	
Wind speed (m/s)	0.32	0.46	0.35	0.17	0.13	

Concerning the operating parameters of the experimental GTC, the focused was on the temperature difference between the collector outlet air temperature and collector inlet air temperature ($\Delta T_{out\text{-}in}$) and the mean absorber temperature (T_{plate}), under different air flow rates (see Table 3).

Based on data in Table 3, it can be noticed that the air heating within the experimental GTC decreases almost linearly with the increase of the air flow, this being more obvious in the case of the configuration with a distance of 30 mm between the glazing and absorber. These findings are also confirmed by the results of Leon and Kumar[17].

Table 3. GTC test parameters (1:10 p.m. to 2:10 p.m.)

30 mm glazing - perforated plate						
Parameter / Air flow rate ($m^3/h,m^2$)	79	101.5	125	148	177	198.5
$\Delta T_{out\text{-}in}$ (°C)	18.1	13.9	13.4	12.6	11.2	10.2
T_{plate} (°C)	57.8	54.6	53.3	48.7	41.5	39.5

50 mm glazing - perforated plate

Parameter / Air flow rate ($m^3/h,m^2$)	77	102.5	127	151	175
ΔT_{out-in} (°C)	13.2	9.6	9.6	8.1	5.4
T_{plate} (°C)	52.7	48.9	44.9	43.9	39.3

It is also found that, for the same air flows, the air passing through the experimental GTC is heated by about 4-5ºC more in the case of a solar collector with a distance between the glazing and absorber of 30 mm, compared to the configuration with a distance of 50 mm. On the other hand, it should be noted that during the tests with the configuration of 30 mm, the average solar radiation was higher (760.2 W/m^2 compared to 665.9 W/m^2).

According to values in Table 3, the same observations apply to the evolution of plate temperature with air flow, linear dependence being even more pronounced. Similarly, higher temperatures of the perforated absorber are recorded in the case of a distance of 30 cm between the glass and the plate, but it must also be taken into account that during the tests for this configuration the average intensity of the solar radiation was higher by approximately 100 W/m^2, as mentioned above.

Finally, in order to assess the performance of the experimental GTC, the efficiency of the solar collector was determined on the basis of experimental data.

The heat exchange efficiency within an air solar collector can be expressed as the following formula[18]:

$$\varepsilon_{HX} = \frac{T_{air-out} - T_{amb}}{T_p - T_{amb}} \quad (1)$$

where $T_{air\text{-}out}$ is the air outlet temperature (K), T_{amb} is the ambient air temperature (K), and T_p is the absorber (plate) surface temperature.

The values obtained based on Eq. (1) for different air flow rates are shown in Figure 3. It can be observed that the efficiency of the heat transfer within the experimental GTC is improved in the case of a smaller distance between the glass and the absorber. On the other hand, for the configuration with 30 mm between the glazing and the perforated plate, the heat transfer efficiency is constant around 50-55%, regardless of the air flow through the air solar collector.

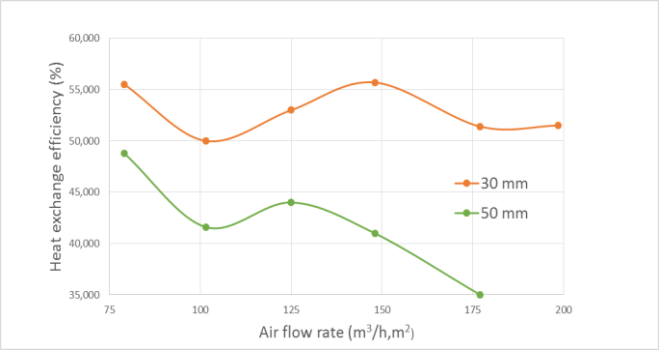

Figure 2. Heat exchange efficiency of the experimental GTC for the two configurations taken into account: distance of 30 mm and 50 mm between the glazing and absorber

The global efficiency of the experimental GTC was judged based on the following expression[13]:

$$\eta = \frac{c_{p,air} m_{air} \left(T_{air-out} - T_{amb}\right)}{I_S A_{abs}} \quad (2)$$

where $c_{p,air}$ is the specific heat of air (J/kg°C), m_{air} is the mass flow rate of air through the collector (kg/s), I_S is the intensity of the solar radiation, and A_{abs} is the absorber area of the air solar collector.

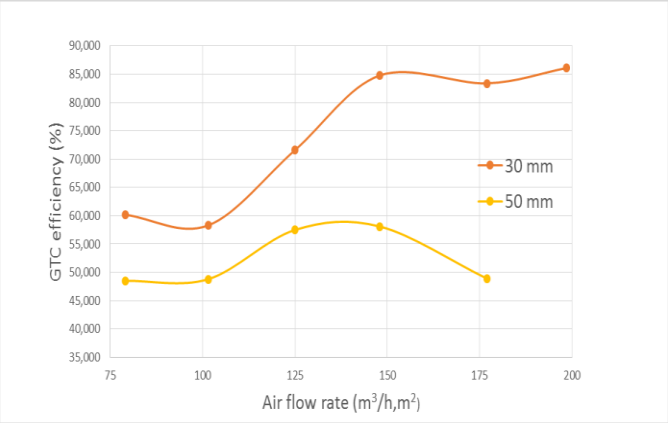

Figure 3. GTC efficiency for the two configurations taken into account: distance of 30 mm and 50 mm between the glazing and absorber

The comparison of GTC efficiency for the two configurations taken into account is given in Figure 4. Based on the results achieved, it can be concluded, also in this case, that the configuration with a smaller distance between the glass and the absorber is much more efficient, for all the air flow rates taken into account.

4. Discussion

The results obtained by testing the experimental GTC proposed in this study show the potential of such solutions for heating the air in the ventilation systems of the buildings. Moreover, the existence of the glazed surface considerably reduces the negative impact of wind velocity on the overall efficiency of air solar collectors, as indicated also by other studies[19, 20]. As a result, this configuration of GTC can be applied with good results to space heating and ventilation in cold (and even windy) climate, as also previously proved by Gao et al. [16]. On the other hand, the results show that the best solution among the tested configurations is with 30 mm distance between the glazing and absorber, no matter what the air flow rate is.

The efficiency of the GTC in this case is 16-19% higher for air flow rates around 100 m3/h,m2 and even 30-40% higher for air flow rates around 150-200 m3/h, m2 – compared to configurations with larger distance between the glazing and absorber. Nevertheless, these findings should be judged by taking into account the influence of different weather conditions, being impossible to keep stable outdoor conditions throughout all the experimental campaigns.

5. Conclusions

The experimental GTC system taken into consideration in this work has allowed to determine the best configuration in order to be implemented in future research concerning “intelligent façades”. Starting from this configuration, inertial elements can be integrated within the GTC system in order to enhance its performance (e.g. phase change materials).

In addition, the results issued from this study can be used to validate numerical models concerning the simulation of thermal behavior of air solar collectors. In fact, CFD (Computational Fluid Dynamics) models are already being developed at the moment for the experimental configurations presented in this paper.

Acknowledgement

This study was financed by Romanian National Authority for Scientific Research, project CIA-CLIM “Smart buildings adaptable to the climate change effects” PN-III-P1-1.2-PCCDI-2017-0391.

References

1. Reichl, C., et al., *Comparison of modelled heat transfer and fluid dynamics of a flat plate solar air heating collector towards experimental data.* Solar Energy, 2015. **120**: p. 450-463.
2. Goyal, R.K., G.N. Tiwari, and H.P. Garg, *Effect of thermal storage on the performance of an air collector: A periodic analysis.* Energy Conversion and Management, 1998. **39**(3–4): p. 193-202.

3. Bejan, A.-S., et al., *Air solar collectors in building use - A review.* E3S Web Conf., 2018. **32**.
4. Nkwetta, D.N. and F. Haghighat, *Thermal energy storage with phase change material—A state-of-the art review.* Sustainable Cities and Society, 2014. **10**: p. 87-100.
5. Zhang, T., et al., *The application of air layers in building envelopes: A review.* Applied Energy, 2016. **165**: p. 707-734.
6. Rosaria Ciriminna, F.M., Mario Pecoraino, Mario Pagliaro, *Solar Air Heating and Ventilation in Buildings: A Key Component in the Forthcoming Renewable Energy Mix.* Energy Technology, 2017. **5**: p. 1-9.
7. Paya-Marin, M.A., et al., *Large scale test of a novel back-pass non-perforated unglazed solar air collector.* Renewable Energy, 2015. **83**: p. 871-880.
8. Hami, K., B. Draoui, and O. Hami, *The thermal performances of a solar wall.* Energy, 2012. **39**(1): p. 11-16.
9. Shukla, A., et al., *A state of art review on the performance of transpired solar collector.* Renewable and Sustainable Energy Reviews, 2012. **16**(6): p. 3975-3985.
10. Croitoru, C., et al., *Thermal Evaluation of an Innovative Type of Unglazed Solar Collector for Air Preheating.* Energy Procedia, 2016. **85**: p. 149-155.
11. Croitoru, C.V., et al., *Thermodynamic investigation on an innovative unglazed transpired solar collector.* Solar Energy, 2016. **131**: p. 21-29.
12. Tajdaran, S., et al., *Geometrical optimisation of Transpired Solar Collectors using design of experiments and computational fluid dynamics.* Solar Energy, 2020. **197**: p. 527-537.
13. Wang, D., et al., *Experimental study on heating characteristics and parameter optimization of transpired solar collectors.* Applied Energy, 2019. **238**: p. 534-546.
14. Vaziri, R., M. Ilkan, and F. Egelioglu, *Experimental performance of perforated glazed solar air heaters and unglazed transpired solar air heater.* Solar Energy, 2015. **119**: p. 251-260.
15. Gao, M., et al., *A study on thermal performance of a novel glazed transpired solar collector with perforating corrugated plate.* Journal of Cleaner Production, 2020. **257**: p. 120443.
16. Gao, L., H. Bai, and S. Mao, *Potential application of glazed transpired collectors to space heating in cold climates.* Energy conversion and manag., 2014. **77**: p. 690-699.
17. Leon, M.A. and S. Kumar, *Mathematical modeling and thermal performance analysis of unglazed transpired solar collectors.* Solar Energy, 2007. **81**(1): p. 62-75.
18. Moon, B.E., et al., *Evaluation of thermal performance through development of an unglazed transpired collector control system in experimental pig barns.* Solar Energy, 2017. **157**: p. 201-215.
19. Li, X., C. Li, and B. Li, *Net heat gain assessment on a glazed transpired solar air collector with slit-like perforations.* Applied Thermal Engineering, 2016. **99**: p. 1-10.
20. Zheng, W., et al., *Thermal characteristics of a glazed transpired solar collector with perforating corrugated plate in cold regions.* Energy, 2016. **109**: p. 781-790.